TISSUE ENGINEERING: Part C
Volume 16, Number 2, 2010

DOI: 10.1089/ten.tec.2009.0248

A Hollow Sphere Soft Lithography Approach for Long-Term Hanging Drop Methods

Won Gu Lee, Ph.D.,[1,2] Daniel Ortmann, M.S.,[1–3] Matthew J. Hancock, Ph.D.,[1,2] Hojae Bae, Ph.D.,[1,2] and Ali Khademhosseini, Ph.D.[1,2]

In conventional hanging drop (HD) methods, embryonic stem cell aggregates or embryoid bodies (EBs) are often maintained in small inverted droplets. Gravity limits the volumes of these droplets to less than 50 μL, and hence such cell cultures can only be sustained for a few days without frequent media changes. Here we present a new approach to performing long-term HD methods (10–15 days) that can provide larger media reservoirs in a HD format to maintain more consistent culture media conditions. To implement this approach, we fabricated hollow sphere (HS) structures by injecting liquid drops into noncured poly(dimethylsiloxane) mixtures. These structures served as cell culture chambers with large media volumes (500 μL in each sphere) where EBs could grow without media depletion. The results showed that the sizes of the EBs cultured in the HS structures in a long-term HD format were approximately twice those of conventional HD methods after 10 days in culture. Further, HS cultures showed multilineage differentiation, similar to EBs cultured in the HD method. Due to its ease of fabrication and enhanced features, this approach may be of potential benefit as a stem cell culture method for regenerative medicine.

Introduction

Embryonic stem cells (ESCs) hold great potential for generating various cell types for cell therapies and tissue engineering.[1–4] Many approaches for developing effective differentiation protocols involve the formation of three-dimensional (3D) cell aggregates called embryoid bodies (EBs) that contain cells of all germ layers.[5–7] In these systems, ESCs are typically cultured in suspension (i.e., low-attachment) dishes.[8,9] The cells in these cultures form EBs that initiate developmental processes and generate derivatives of the endoderm, mesoderm, and ectoderm.[10,11] Although simple, these methods generate wide ranges of EB sizes,[12,13] which affect the direction of ESC differentiation.[14,15] For example, recently it has been reported that EB size affects chondrogenesis of mouse ESCs.[16] Efforts to control EB size include the popular hanging drop (HD) method, in which ESCs are suspended in 20–25 μL droplets of medium on the lid of a Petri dish.[17,18] When the lid is inverted, the ESCs settle under gravity and aggregate on the menisci of the hanging droplets. EB sizes are controlled by adjusting the droplet volume and cell concentration. ESCs can form aggregates at the air–water interface and therefore maintain their spherical shapes. The disadvantage of HD methods is that gravity limits the droplet volume to less than 50 μL, so that nutrients are depleted within 2–3 days. To sustain growth rates, periodic replenishment is necessary, which is not only laborious but also can easily disturb the autocrine and paracrine signaling in the EBs and upset the equilibrium ambient conditions within the drops. Other approaches to control EB size include microwell structures,[13,19] stirred vessel bioreactors,[20] and rotary suspension cultures.[21] In the latter two methods, aggregation, proliferation, and differentiation may be altered by shear stresses and hydrodynamic forces.[22] In the microwell system, EBs grow until they reach the border of the well and are then limited in their proliferation, presumably due to mechanical confinement in the wells.

In this study, we present a new cell culture method using hollow spheres (HSs) that enables the formation and growth of individual EBs at liquid–gas interfaces in a long-term HD format for more than 10 days. Through this approach, we found that the EBs cultured in the HS structures maintained their ability to differentiate in a multilineage manner. A soft lithographic approach was developed using liquid drops to form HS structures in a noncured poly(dimethylsiloxane) (PDMS) mixture. Each HS structure has a small opening that

[1]Department of Medicine, Center for Biomedical Engineering, Harvard Medical School, Brigham and Women's Hospital, Boston, Massachusetts.
[2]Harvard–MIT Division of Health Sciences and Technology, Massachusetts Institute of Technology, Cambridge, Massachusetts.
[3]Department of Internal Medicine II–Cardiology, University of Ulm, Ulm, Germany.

serves as an inlet port for EBs within a HD, and, when inverted, holds a meniscus where EBs form, similar to HD methods. Medium replenishment is also facilitated, depending on the particular experimental design, which allows for even longer culture durations (>15 days). The geometries of the HDs attached to the rim of HSs were analyzed and shown to agree with existing theory. This method is cost effective, scalable, simple to fabricate without the need for microfabricated 3D replica molds, enables ESC aggregates to grow larger (up to 1000 μm), and generates chambers that hold large volumes of fluid (500 μL in each sphere).

Materials and Methods

Culture device design and fabrication

The overall fabrication scheme for generating the HS geometry is illustrated in Figure 1. The liquid spheres were created in a cured high-viscosity PDMS solution (Sylgard 184; Dow Corning, Midland, MI). The specific gravities of the PDMS monomer and curing agent (in liquid form) are 1.11 and 1.03, respectively, and their viscosities at 24°C are 50 and 1.1 $cm^2\ s^{-1}$, respectively. Therefore, distilled water (DW) can be used to generate liquid spheres that can be placed beneath the PDMS air surface without sinking to the bottom. To fabricate the HSs, a solution containing the PDMS mixture (10:1 ratio) was poured into a culture dish. A controlled volume of liquid was then loaded onto the PDMS mixture using a pipette. A thin PDMS membrane was automatically created at the top of the immersed liquid drop. The PDMS was then cured in an oven at 80°C for 1 h or at room temperature for 1 day. To make the entrance hole of the HS, the thin membrane was easily trimmed along its rim by using sharp-edged tweezers. After the thin membrane was gently detached, the liquid was removed with a pipette. The size of the opening and the liquid volume injected into the HS determine the shape of the meniscus when the HS is inverted (Fig. 2B; Supplemental Figs. S1B, S2A, and S2C, available online at www.liebertonline.com). For most cell culture studies, the HS was filled with 500 μL of the cell medium containing 300 cells. The HSs may be created with volumes ranging from 0.5 to 500 μL. In our experiments, we selected 500 μL for long-term HD methods. A more detailed explanation on methodology is given in the Results and Discussion section.

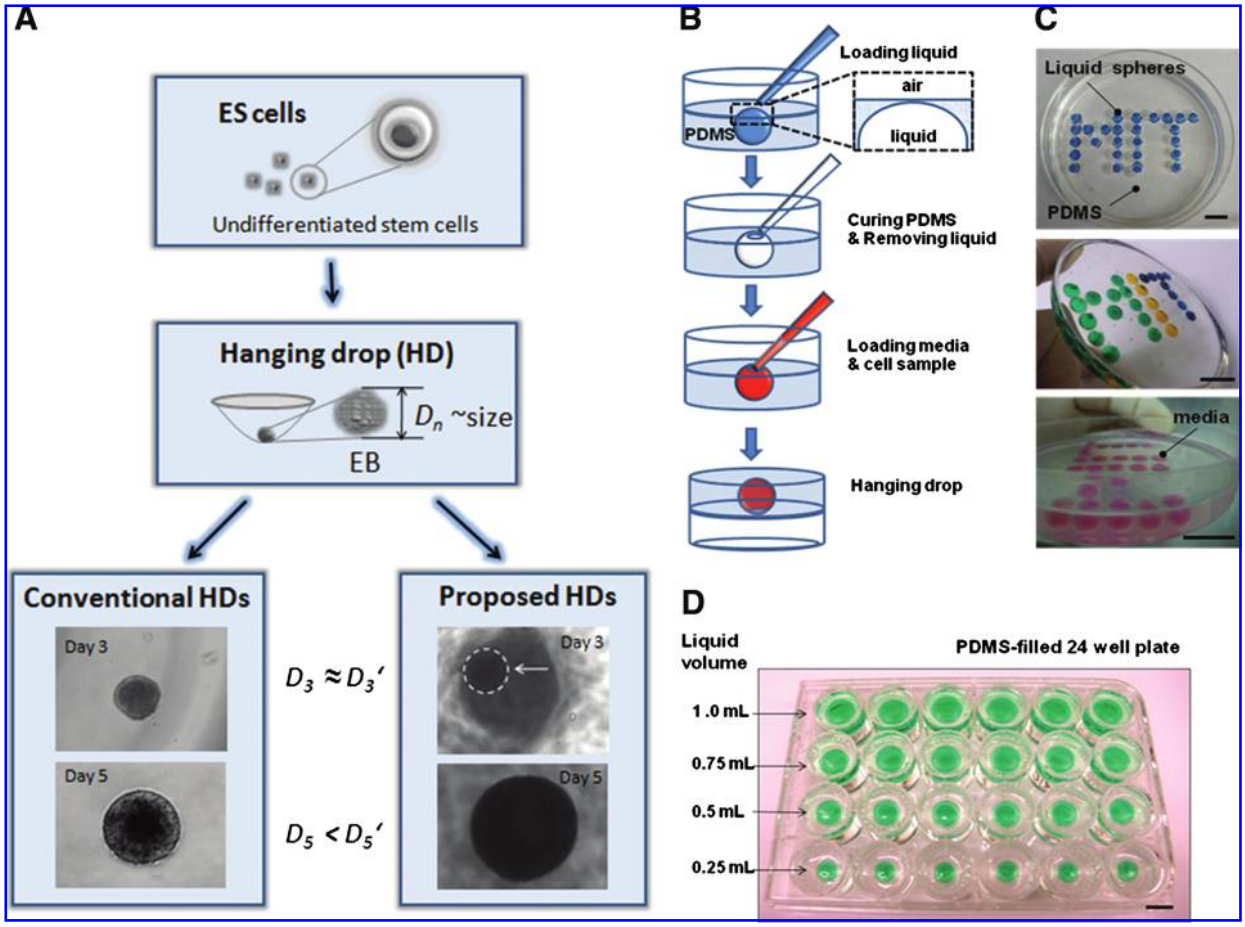

FIG. 1. Schematic for the HS soft lithography process for long-term HD culture. (**A**) Schematic for the HS culturing process. D_n is the diameter of EB corresponding to the *n*-day culture. (**B**) Fabrication scheme for generating HS mesostructures. (**C**) Design and fabrication of the "MIT" logo filled with DW and different food-coloring dyes. Scale bar is 1 cm. (**D**) Optimization of the HS size by using liquid volumes that range from 0.25 to 1.0 mL. Scale bar is 1 cm. HD, hanging drop; HS, hollow sphere; EB, embryoid body; DW, distilled water. Color images available online at www.liebertonline.com/ten.

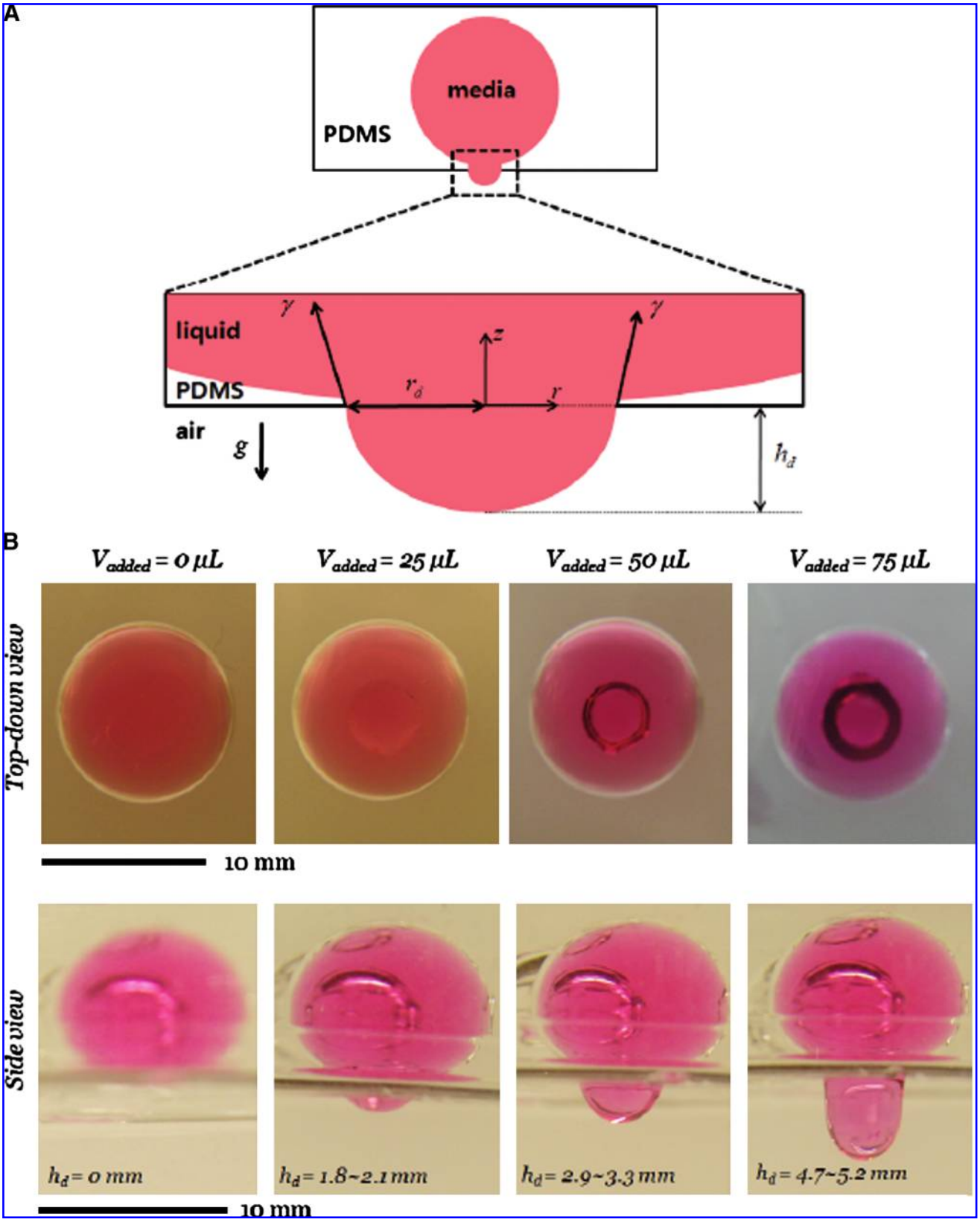

FIG. 2. Evaluation of the effect of gravity on the HD curvature. (**A**) Schematic of salient parameters for HD formation under gravity. (**B**) Photographs of HDs of media under HSs for different added volumes: 0, 25, 50, and 75 μL. Bubble-like reflections are diffracted images of other empty HSs. No bubbles are present inside fluid-filled HSs. Color images available online at www.liebertonline.com/ten.

Measurement of sphericity of HS structure in the fabricated device

To examine the sphericity of the fabricated HSs, Wadell's sphericity formula was employed,

$$\Psi(sphericity) = \frac{2\sqrt[3]{ab^2}}{a + \frac{b^2}{\sqrt{a^2+b^2}} \ln\left(\frac{a+\sqrt{a^2-b^2}}{b}\right)}, \quad (1)$$

where a and b are the measured semi-major and semi-minor axis of the created HSs, respectively.

Characterization pendant drop meniscus

When the HS is filled and inverted, a pendant drop forms and hangs from the HS entrance. The shape of the pendant drop's axis-symmetric meniscus was first studied by Young and Laplace in 1805.[23,24] The problem is scaled by the capillary length, $l_c = \sqrt{\gamma/\rho g}$, over which gravitational and surface tension forces balance. For DW or sterile cell media,[25,26] $\gamma = 72$ dynes cm^{-1}, $\rho = 1.0$ g cm^{-3}, and $l_c = 2.7$ mm; for cell media with cells,[25–27] $\gamma = 39$–49 dynes cm^{-1}, $\rho = 1.005$ g cm^{-3}, and $l_c = 2.0$–2.2 mm. The relative importance of gravity and surface tension is quantified by the (dimensionless) *Bond* number

$$B_0 = \frac{\text{gravitational force}}{\text{surface tension force}} \sim \frac{\rho g r_d^2}{\gamma} = \left(\frac{r_d}{l_c}\right)^2, \quad (2)$$

where r_d is the base radius of the pendant drops (Fig. 2). In our experiments, B_0 ranged from 0.01 to 1.2. Pendant drop geometry and, in particular, the relation between the drop height, volume, and base radius (equal here to the HS entrance radius) are well understood,[28–32] and efficient computational methods for the relevant differential equations are available.[33] For sufficiently small drop volumes, the meniscus shape is approximately a spherical cap with volume V_{cap} given in terms of the height h_d and base radius r_d via

$$V_{cap} = \frac{\pi}{6} h_d \left(3r_d^2 + h_d^2\right). \quad (3)$$

Long-term HD method using HS structures

The HSs in PDMS were washed with phosphate-buffered saline (PBS) and filled with 20% fetal bovine serum (FBS) containing medium until the desired pendant drop curvature was reached. The degree of curvature is determined by the volumes of the HS and the injected medium. From each HS, 25 μL medium was removed and then replaced with 25 μL of an ESC suspension solution. To ensure that the initial cell counts in both the HD and HS experiments were the same, the same cell solution was used. The HS device was then inverted and cultured under the same conditions as the HD cultures.

Long-term HD method by modifying conventional HDs

When ESCs were cultured and reached the desired density (3×10^2 cells per drop) in the flask, they were passaged or used for an experiment. After aspirating the medium, the ESCs were washed with PBS and then treated with trypsin for approximately 3 min to detach them from the dish. Trypsinization was halted by adding serum-containing medium. The cells were then transferred to a 15 mL falcon tube and centrifuged at 1000 rpm for 5 min. The solution was then aspirated, and the cells were resuspended in a solution containing 20% FBS at the desired cell density. A multichannel pipette was used to generate 25 μL drops on the lid of an 8.5-cm Petri dish (Beckton–Dickinson, Franklin Lakes, NJ). The dish was inverted, and 10 mL of PBS was put into the bottom to minimize evaporation from the HDs. The dishes were then kept in a humidified incubator at 5% CO_2 and 37°C for the duration of the experiment (85–95% relative humidity). In most cases, the medium in the HDs was refilled each day. Therefore, the dishes were removed from the incubator and the lids were inverted. The medium was carefully removed from the rim of each droplet by using a pipette. Fresh medium was then added, and the dishes were returned to the incubator.

Culture of mouse ESCs and EBs

Mouse ESCs (R1 cell line) and ESCs that express a reporter gene for goosecoid (Gsc) were cultured in tissue culture flasks at 5% CO_2 and 37°C humidified incubators and passaged every other day. The *Gsc* gene is an ideal marker for mesendoderm, where Gsc-positive cells express green fluorescent protein.[34] The cell culture medium consisted of high glucose Dulbecco's modified Eagles medium (Gibco, Carlsbad, CA) supplemented with 10% (v/v) FBS (Gibco), 100 U mL^{-1} penicillin and 100 mg mL^{-1} streptomycin (Gibco), 1 mM L-glutamine (Gibco), 0.1 mM β-mercaptoethanol (Sigma, St. Louis, MO), and 1000 U mL^{-1} of leukemia-inhibitory factor (Chemicon, Billerica, MA).

Reverse transcriptase–polymerase chain reaction

Total RNA was extracted from EBs harvested from two different EB culture methods using TRIZOL reagent (Invitrogen, Carlsbad, CA) according to the manufacturer's instructions. First-strand cDNA synthesis and PCR amplification were performed in a single step using the SuperScript™ III One-step RT-PCR System with Platinum® Taq kit (Invitrogen) according to the manufacturer's instructions. cDNA synthesis was performed with 100 ng total RNA and was allowed to proceed at 53°C for 25 min. After an initial denaturation step at 94°C, several cycles of PCR were carried out using a PTC-100TM thermal cycler (MJ Research, Waltham, MA) under the following conditions: 15 s denaturing at 95°C, 30 s specific primer annealing temperature, and 45 s extension at 68°C. After amplification, PCR products were loaded on 2% (w/w) agarose gels containing ethidium bromide at a concentration of 0.5 μg·mL^{-1}. Digital images of the fluorescently labeled amplification products were captured using the Gel Logic 100 Imaging System with Molecular Imaging Software (Eastman Kodak Company, Rochester, NY). For quantification, images were analyzed using *Image J* software, and background noise was subtracted from the intensity values of the individual bands. The expression of the housekeeping gene *GAPDH* served as an internal RNA standard to which the expression levels of the investigated genes were normalized. Each expression level was determined as the mean if measurements were obtained from two reverse transcriptase–polymerase chain reaction (RT-PCR)

experiments from independent EB cultures. The primers used for evaluating gene expression profile of ESC differentiation are detailed in Supplemental Table S1 (available online at www.liebertonline.com).

Immunostaining of cultured EBs

Mouse ESC differentiation (i.e., three germ layer formation) was confirmed by immunocytochemical staining. For antibody staining, EBs were washed twice with 1× PBS and fixed with 4% paraformaldehyde (Sigma) in 1× PBS at room temperature for 30 min. After incubation, the samples were washed three times with 1× PBS. Then 0.1% Triton X-100 (Sigma) in PBS was added to permeabilize cells for intracellular staining. Finally, 10% (w/v) normal goat serum (Invitrogen) in PBS was added to block nonspecific antibody binding. The primary antibodies, anti-brachyury (goat polyclonal) (Santa Cruz Biotechnology, Santa Cruz, CA), anti-nestin (goat polyclonal) (Santa Cruz Biotechnology), and anti-α-fetoprotein (AFP-specific mouse monoclonal) (R&D Systems, Minneapolis, MN), were added to each sample and then incubated at 4°C overnight. After washing three times with PBS, the secondary antibodies were added and incubated in blocking solution at room temperature for 1 h. The types of secondary antibodies used were mouse anti-goat IgG-R (for brachyury and nestin) and goat anti-mouse IgM–R-phycoerythrin conjugates (for AFP). After washing three times with 1× PBS, the cells were counter-stained with 4′,6-diamidino-2-phenylindole (DAPI) (Vecta Shield–Fisher Scientific, Burlingame, CA) for nuclei staining at room temperature for 1 h.

Fluorescence imaging and data analysis

Phase-contrast and fluorescence images of EBs were taken every other day under a standard inverted fluorescent microscope (Nikon, TE2000, Melville, NY) with a 10× objective. Others have reported that the central cores of EBs can show nonspecific staining.[15] For the purpose of imaging, the HD dishes were inverted to bring the HDs sufficiently close to the objective. In the PDMS device, images could be taken directly, without inversion of the plate. The diameters of EBs were then measured using *Image J* software developed at the National Institute of Health.

Statistical analysis

The Student paired *t*-test was performed for different EB samples cultured in conventional HDs and HSs. *p*-values <0.05 were considered statistically significant. Values are reported as the mean ± standard deviation.

Results and Discussion

The current study has two aims: (i) to develop a new method for generating 3D HS culture chambers and (ii) to demonstrate their feasibility for long-term HD cultures (Fig. 1A).

HS soft lithography: Design, fabrication, and characterization

The HS geometry was characterized, and the resulting HD methods were analyzed both experimentally and theoretically and compared with conventional HD methods. To fabricate a HS, water was injected below the surface of the noncured PDMS mixture. When injected into the PDMS solution, water forms a spherical or elliptical drop within the solution. In our experiments, water was immiscible in the PDMS solution and remains stable during the PDMS curing. However, we found that after the PDMS was cured it could absorb a small quantity of water and swell. Following injection into the PDMS solution, the liquid sphere floats partially submerged since the density of water is less than that of PDMS. Initially, a thin viscous lubricating layer of PDMS solution coats the top of the sphere and slowly drains. Depending on the relative speeds of drainage and solidification, the thin layer may remain intact or develop a hole at the pinnacle. For HS volumes larger than 600 μL, entrance holes with diameters larger than 8–9 mm formed due to drainage (data not shown). The HSs could therefore not support stable pendant drops when inverted. The HS geometry may be modified by using a range of liquid volumes to fabricate the spheres (between 0.5 and 600 μL). In this study, we selected 500 μL to perform long-term HD experiments. The HS geometry was visualized by filling the HSs with DW containing food-coloring dye (Fig. 1B) and was quantified by using either direct visualization (Supplemental Fig. S1A) or, for volumes less than 2.5 μL, by microscopy (Supplemental Fig. S1B). For each HS with volume less than 2.5 μL, we observed an opening (white round area) at the pinnacle of the thin layer and a thin "white-ring" shape between the center and the rim (Supplemental Fig. S1B) caused by light diffraction in the HS under an inverted microscope. Further, stable pendant drops were successfully produced within HSs of various volumes.

Our fabrication method enables liquid spheres in PDMS solution to be arranged in specific patterns, such as the "MIT" logo (Fig. 1C). In some cases, slow motion of the HSs was observed during the fabrication. This may be due to interfacial forces, convection, or the density difference of the HSs during PDMS solidification. For ESC experiments, we used 500 μL HSs since they offer reproducible results for HD methods and large media volumes for nutrient storage (Fig. 1D). The HSs in our device were filled with medium and then loaded with ESCs at a concentration of 600 cells mL^{-1}. The medium volume was approximately 20 times greater than that of the droplets used in conventional HD methods, providing enough nutrients for at least 10 days of culture.

A key requirement of HD methods is to be able to generate a large number of drops per unit area. In our case we used standard 24-well plates as array containers for the cured PDMS (10:1 ratio) prepolymer solution. The fabricated HSs were characterized based on their sphericity and formation efficiency. The formation efficiency is defined as the ratio of the number of created HSs to the total number of stable liquid drops. The sphericities of the fabricated HSs were 0.9965 ± 0.037 (mean ± standard deviation) (Supplemental Fig. S2). For HS volumes greater than 5.0 μL, the HS formation efficiency was 100%, and all measured sphericities were at least 0.988 (Supplemental Fig. S2). For HS volumes less than 5.0 μL, microscopic images were taken and then quantified (Supplemental Fig. S1). Our fabrication method produced uniformly round HSs with a wide range of volumes. A summary of the characterization of the HS geometry is given for various liquid volumes (Supplemental Fig. S2).

The toxicity of PDMS residue may affect long-term (greater than 1 week) cell culturing in PDMS microstructures.[35]

Specifically, the toxicity of PDMS (e.g., Sylgard 184) may be caused by the base monomer, tetra (trimethylsiloxy) silane, and the curing agent, tetramethyl tetravinyl cyclotetrasiloxane. In our experiments, the toxic effects of the PDMS monomer residue on cell culture were decreased because the device was allowed to incubate overnight in an aqueous solution, washed with 70% ethanol, and then oven dried at 80°C for 1 h. After washing twice with DW and removing all liquids from the HS structures, the device was again thoroughly oven dried at 80°C for 6 h. Interestingly, we also found that the volume of the HS structure decreased slightly after this detoxification process. For instance, the 500 μL liquid capacity decreased to ~480 to 490 μL (data not shown). In addition, since the HS is a mesoscale structure, the toxicity of the surface of the PDMS structure is expected to be mild and may be mitigated by exposing the HS surface to a liquid and washing before an experiment.

To demonstrate the application of HSs for HD methods, we measured the height h_d of HDs versus the liquid volumes added to the HSs. We obtained different shapes and sizes of stable pendant drops for an HS volume of 500 μL (Fig. 2A). The listed HS volumes indicate the fluid volumes used to create the HS. For HSs larger than 100 μL, filling a cured HS with its listed volume overfilled it, thereby creating a pendant drop on inversion. The size of the HD may be increased by adding fluid beyond the listed volume to the HS, denoted by "added volume" (Fig. 2B). For the purposes of our HD experiments, the drop volume V_d was measured by initially filling an HS to a level flush with the entrance, and then measuring the volume V_d added beyond that for the pendant drop (Fig. 3). Our experiments show that HSs offer great potential for generating large pendant drops.

Comparison to pendant drop theory

To generalize our observations, we compare our HD measurements to the established theory of pendant drops, reviewed above. Numerical simulations of drop height versus volume for various HS entrance radii are given in Figure 3A for a wider range of parameters than those given previously.[29,30] The calculation follows the formulation given by Rio and Neumann.[33] Measurements of the height and volume of pendant drops hanging from HSs filled with DW and cell media are included in Figure 3A, and are in general agreement with the theory. The discrepancy between theory and experimental results may stem from minor deformation of the PDMS slab containing the HSs, unsupported for the purposes of measurements, which slightly increased the HS volumes and reduced the HD volumes. Various factors limit the size of pendant drops. Pendant drops are stable only if the orifices under which they hang have radii less than 3.219 l_c.[30,32] A horizontal circular planar interface separating water over air is stable if its radius is less than 2.405 l_c.[29,30] These theoretical findings rationalize our experimental observation that inverted HSs with entrance radii larger than approximately 8–9 mm could not support pendant drops. Next, the drop's weight must be supported vertically by surface tension and pressure forces. The maximum pendant drop volume and height have been tabulated for various parameter ranges.[28,29] For drops whose radius is small relative to the capillary length, an asymptotic formula for the maximum volume has been given.[31] In Figure 3B, pendant drop volumes, including

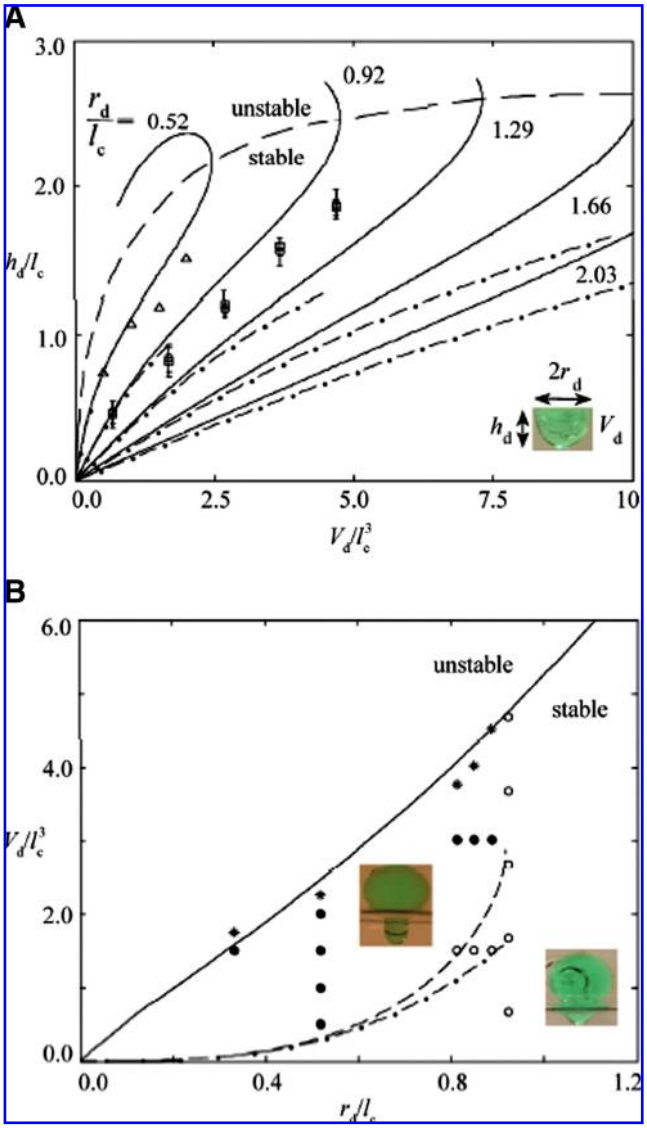

FIG. 3. Characterization of HD shape from pendant drop theory. (**A**) Dependence of pendant drop height h_d on volume V_d, scaled by the capillary length l_c, for fixed base radius r_d. Numbers adjacent to solid lines indicate r_d/l_c; for DW, these correspond to $r_d = 1.4$, 2.5, 3.5, 4.5, and 5.5 mm, increasing left to right, since $l_c = 2.7$ mm. (– –) Theoretical maximum drop height of Ref. 29 and (–·–) spherical cap height from Equation (3). Experimental measurements and error bars shown for (Δ) DW with $r_d = 1.4$ mm, (○) DW, and (□) cell media for $r_d = 2.5$ mm. (**B**) Dependence of pendant drop shape on volume V_d and base radius r_d. (—) Theoretical maximum drop volume of Ref. 29 below which drops are stable. (– –) Phase boundary between bulbous (above) and cap-shaped (below) drops. (–·–) Hemisphere volume plotted for comparison. Insets show typical bulbous and cap-shaped pendant drops hanging below HSs. Experimental measurements for pendant drops below HSs filled with DW shown for (•) bulbous drops, (○) cap-shaped drops, and (*) drops with maximum volume for a given base radius. Color images available online at www.liebertonline.com/ten.

the maximum realizable, are plotted versus the orifice radius r_d. The theoretical prediction of maximum volume is included for comparison and agrees well with our measurements.[29] The parameter domain is divided into three regions: stable bulbous drops, stable cap-shaped drops, and a region that does not result in stable drops. The phase boundary separating the two drop types is calculated using the formulation for cap-shaped drops whose meniscus is vertical at the orifice (i.e., the entrance to the HS).[33] The volume of a hemispherical drop, $2\pi r_d^3/3$, is plotted for comparison.

Long-term HD formation

To demonstrate the advantages of the HS approach as a culturing method, EBs were cultured in a HS system and directly compared with the conventional HD method. The HS device consisted of 500 μL HSs with 25 μL drops suspended below (Supplemental Fig. S3). In both the conventional HD and the new HS methods, EBs were formed by the gravity-induced settling of cells to the meniscus. After approximately 4 days of incubator culturing, the EBs in the HDs that were not renourished daily began to lose their integrity by decreasing in diameter and disintegrating (data not shown), and broke into several small satellite aggregates after 5 days of culture. This loss of integrity was probably due to the depletion of the medium ingredients and the accumulation of metabolic substances. Even with periodic medium replenishment, the size of EBs was limited in conventional HD methods. In contrast, the EBs in the HS method continued to grow, indicating that the large reservoir of media contained in the HSs provided more nutrients during EB formation (Fig. 4A). When the initial number of ESCs seeded was increased, the initial diameter of the EBs increased as well as the frequency of multiple EBs forming in one drop (data not shown). The proposed HS device achieved substantially higher EB sizes compared with the conventional HDs with daily renourishment. The EBs grown in the HS reached approximately 1000 μm in diameter within 10 days of culture (Fig. 4A). The HS method does not require the addition of PBS if the relative humidity of the culture

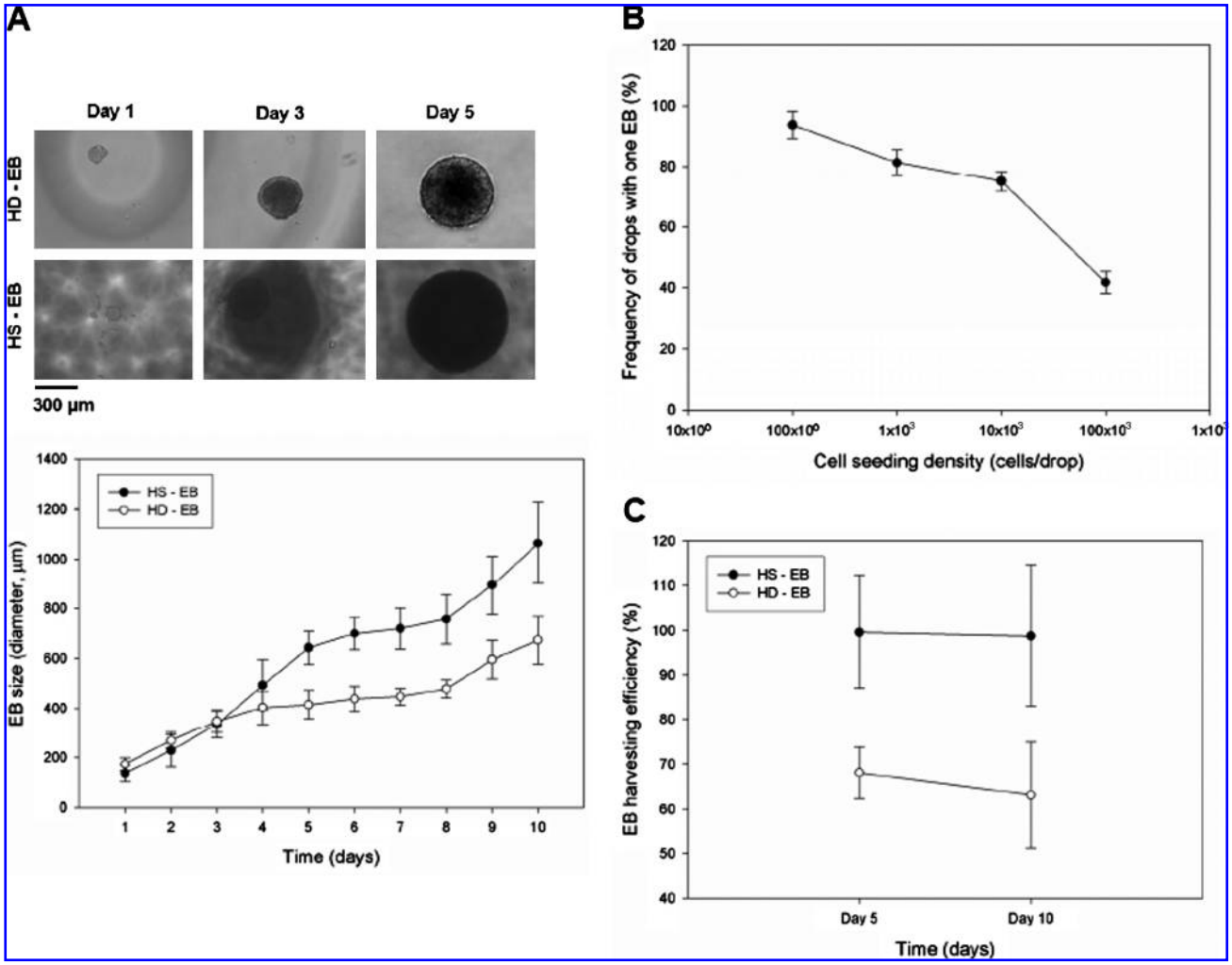

FIG. 4. Comparisons of HS and HD culture systems for EB formation. (**A**) Representative image of HS-EBs to HD-EB for 5 days of EB culture, which compares the size of EB formation between the HS and HD. Scale bar is 300 μm. Cell seeding density is 300 cells per drop. (**B**) Graph for frequency of drops with one EB versus cell seeding density. (**C**) Graph for harvesting efficiency of cultured EBs for the HS and HD methods. Note that conventional HD-EB method requires media replenishment unlike the HS-EB method.

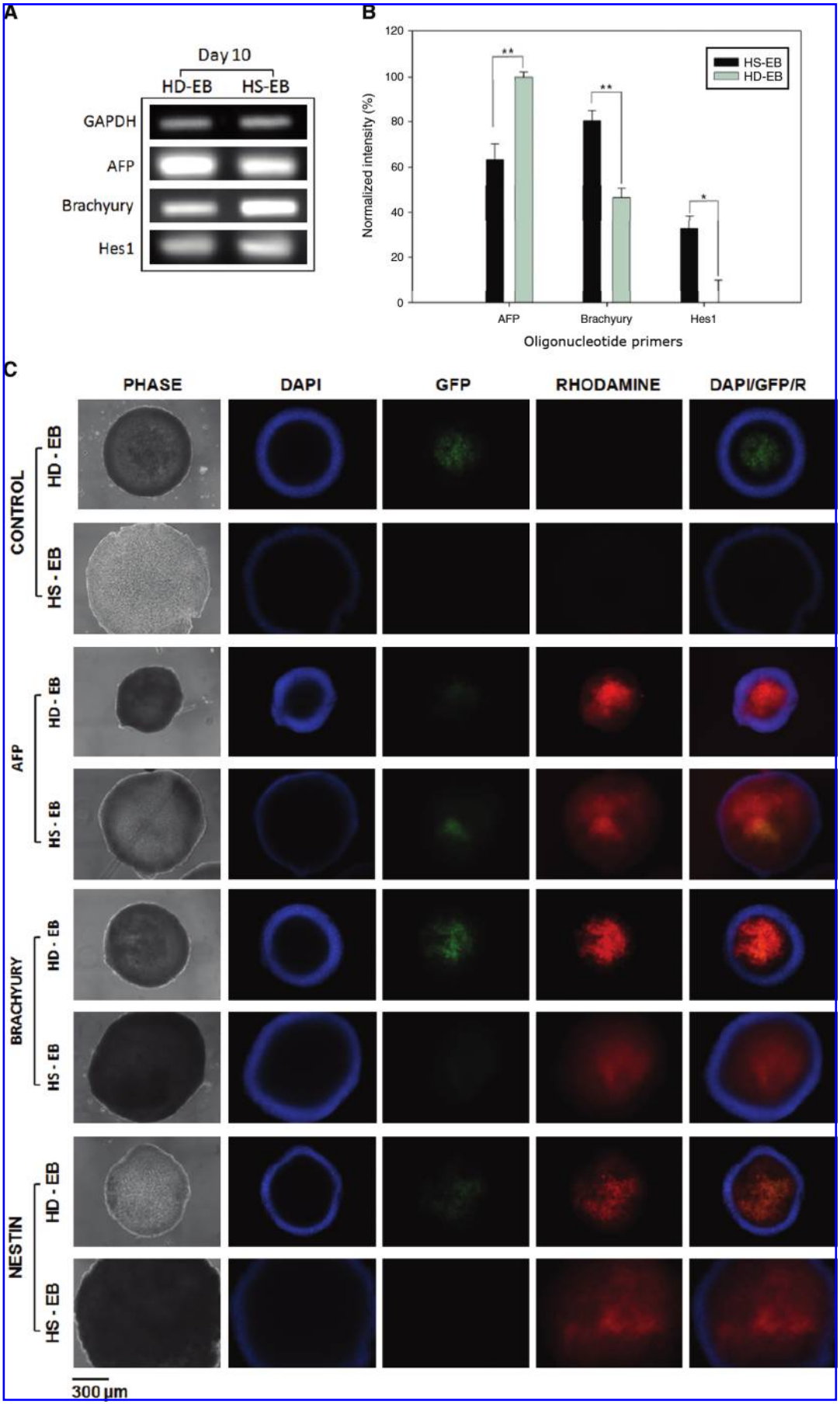
A
Day 10
HD-EB
HS-EB
GAPDH
AFP
Brachyury
Hes1
B
Normalized intensity (%)
HS-EB
HD-EB
AFP
Brachyury
Hes1
Oligonucleotide primers
C
PHASE
DAPI
GFP
RHODAMINE
DAPI/GFP/R
CONTROL
AFP
BRACHYURY
NESTIN
HD - EB
HS - EB
300 μm

Table 1. Characteristics of Various Embryoid Body–Formation Techniques in a Hanging Drop Form

Contents	HD capacity (μL)	HD period (days)	Gravity (g)	Throughput (N)	Single EB formation (%)[b]	Potential pros/cons for long-term HD method	References
Liquid/gas phase[a]							
Traditional HDs	20–50	2	1	24–96	60–71 (mouse)	Pros: user-friendly, media-refillable; cons: limited liquid volume	39, 40, 12
Multiwell chip	10	2–3	1	96	98 ± 3 (mouse)	Pros: rapid, uniform EB formation; cons: limited liquid volume	40
PDMS hollow sphere (HS)	~500	10	1	24–96	98.9 ± 1.7 (mouse)	Pros: long-term HD (gas interface); cons: imaging difficulties (3D geometry)	Present work
Liquid/solid phase							
Polypropylene conical tube (CT)	1000	5	1	24	99.3 ± 1.7 (mouse)	Pros: large media volume; cons: limited use of CT	39
Centrifugal precipitation wells	100	10–12	478	96	95.8 ± 1.6 (human)	Pros: long-term HD (solid interface); cons: unknown effect by centrifuge	41
Polyvinyl carbonate PCR plate	200	4	1	96	94 (mouse)	Pros: simple EB formation; cons: limited use of PCR plate	42

[a]The liquid/gas phase indicates the state of the interface near the ESC aggregates.
[b]Single EB formation denotes frequency of drops with one EB formation (Figure 4B).
HD, hanging drop; EB, embryoid body; PDMS, poly(dimethylsiloxane); PCR, polymerase chain reaction.

environment is adequate. If the relative humidity is not sufficient, PBS may be added to mitigate the effects of unwanted evaporation. In our experiments, a small amount of PBS was added to the HSs once to maintain HDs for more than 10 days. For comparison, in the same culture environment, our conventional HDs required 20 μL of media to be added every other day to endure a 15-day EB culture (Supplemental Figs. S3 and S4). The HS method avoids cumbersome replenishment and still yields a higher harvesting efficiency for EB cultures, defined as the ratio of the number of harvested EBs to the number of initially formed single EBs in each drop (Fig. 4B). The EB harvesting efficiency was measured as 68.13% (HD-EB) and 99.58% (HS-EB) for 5 days of culture and as 63.13% (HD-EB) and 98.75% (HS-EB) for 10 days of culture (Fig. 4C).

To analyze the multilineage differentiation of EBs in both HS and conventional HD cultures, we used RT-PCR and immunocytochemical staining. The RT-PCR data indicated that HS cultures expressed the markers associated with all three germ layers (Fig. 5A). This was also confirmed by immunocytochemical staining images (Fig. 5B). Note that since Gsc-EBs were used for the experiments, the images of green fluorescent protein indicate EB differentiation into mesendoderm tissue. The RT-PCR results show that EBs expressed markers for all three germ layers: *AFP* (endoderm), *brachyury* (mesoderm), and *hes1* (ectoderm). To observe endoderm differentiation at the molecular level, we measured the presence of *AFP*, an endoderm marker that can be useful for late endodermal differentiation and early hepatic expression. During EB formation, yolk sac–like structures increase the gene expression level for *AFP*, causing it to be strongly expressed.[36] In addition, we measured the presence of *brachyury* that is related to the transcription of genes for mesoderm differentiation. A higher expression of *brachyury* was observed for the EBs cultured in the HSs than for those in the conventional HDs. This supports the hypothesis that mesodermal phenotypes can be varied as the size of the EBs increases. Also, we measured the level of expression of *hes1*, which is related to early neural differentiation. A slightly higher expression of *hes1* was observed for the EBs cultured in the HSs compared with EBs in the conventional HDs.

Table 1 outlines the EB formation technique in a HD form. Typical HD methods often require media replenishment after 2–3 days of culture. To avoid frequent media replenishment, the EBs may be grown in suspension cultures. Although suspension cultures are highly scalable, nonoptimal conditions may expose EBs to shear stresses and may result in EB fusing.[13] One alternative not involving HDs is the microwell system, which provides good control of EB formation in a scalable manner. The EBs can be maintained in microwells for at least 2 weeks. However, this method suffers from unwanted cell attachment to the surface of the microwell platform,[19] especially in longer experiments.[37] Culturing EBs

FIG. 5. RT-PCR analysis and immunocytochemical staining images of germ layer markers for 10-day EBs. (**A**) RT-PCR results for *Brachyury* (mesoderm), *AFP* (endoderm), and *Hes1* (ectoderm) for 10-day EB. (**B**) Quantification of the relative expression levels of each gene was made based on measurements of area and intensity, followed by normalization with subtracted background (min–max). RT-PCR experiments were repeated three times. *p*-values (**) are <0.02, and *p*-value (*) is 0.0260. All *p*-values were statistically significant. (**C**) Immunocytochemical staining results for DAPI (blue), green fluorescent protein (green), and rhodamine (red). DAPI imaging: exposure time 50 ms, gain 1; green fluorescent protein imaging: exposure time 1000 ms, gain 8; PE and rhodamine imaging: exposure time 1000 ms, gain 8. RT-PCR, Reverse transcriptase–polymerase chain reaction. Color images available online at www.liebertonline.com/ten.

on liquid–gas interfaces eliminates the attachment problems and allows for free exchange with the gas phase in which the composition may be adjusted to control the EB environment. The EB formation efficiency in the HS platform is comparable to those of HD methods. It is also possible, though not tested experimentally in this study, to fill individual HSs with different substances to test their influence on EB differentiation and development on a single platform. Depending on the number of cells in each HS, the frequency of drops containing one EB is greater than 90%. As the initial cell density increases, so does the tendency to form more than one EB (Fig. 4B). This indicates that the formation efficiency is dependent on the number of cells in each HS. The HS device enables the medium to be replenished for long-duration (e.g., more than 10 days) methods in a HD format. To maintain long-term cultures, renourishment may be required if evaporation occurs, though this may be mitigated using an environmental chamber.[38]

In summary, we have introduced a new approach for creating 3D spherical structures by using HS soft lithography and have outlined a particular biological application, the long-term HD method for basic stem cell research. A large volume HS device enables long-term culture of EBs under persistent conditions and is ideally suited for studies requiring sustained and efficient EB formation and maintenance. The HD method is one of the many applications of the HS fabrication method, which readily allows various sizes and configurations of 3D spherical culture geometries to be generated in a controlled manner. The method is potentially beneficial for producing 3D spherical geometries for cell culture environments and may be applied, for example, to fabricate tissue culture scaffolds requiring 3D spherical geometries.

Conclusions

In this study, we present a method to generate HSs of different sizes and configurations and use these to suspend large volumes of medium against gravity, thereby enabling long-term HD methods. The HS geometries are analyzed and in agreement with existing theory. The abundant nutrient supply contained in the medium enables sustained, high radial expansion of EBs for 10 days or more. The HS approach is simple to fabricate, cost effective, and scalable. Therefore, this approach is potentially beneficial for studying stem cell differentiation and developmental processes by overcoming several limitations of conventional HD methods.

Acknowledgments

The authors thank Dr. S.H. Park of Tufts University for fruitful discussions on EB formation, and Drs. Y.-S. Hwang and W. Sim, Brigham and Women's Hospital, Harvard Medical School for helpful comments on ESC cultures. This work was supported by the National Institutes of Health (DE019024, HL092836, EB007249) and by the German Academic Exchange Service (DAAD). W. G. Lee was partially supported by the Korea Research Foundation Grant funded by the Korean Government (MOEHRD) (KRF-2007–357-D00035).

Author Contributions

W.G.L., D.O., and A.K. conceived this project; W.G.L. designed methodology and fabricated the devices; W.G.L. and D.O. conducted bulk of EB culture experiments; W.G.L. performed immunostaining; H.B. performed RT-PCR; M.J.H. performed the theoretical calculations on pendant drops; W.G.L., D.O., M.J.H. and H.B. analyzed the data. All authors wrote the manuscript and consented to the contents of the final version of the manuscript.

Disclosure Statement

No competing financial interests exist.

References

1. Zandstra, P.W., and Nagy, A. Stem cell bioengineering. Annu Rev Biomed Eng **3,** 275, 2001.
2. Wobus, A.M., and Boheler, K.R. Embryonic stem cells: prospects for developmental biology and cell therapy. Physiol Rev **85,** 635, 2005.
3. Zandstra, P.W. The opportunity of stem cell bioengineering. Biotechnol Bioeng **88,** 263, 2004.
4. Khademhosseini, A., Langer, R., Borenstein, J., and Vacanti, J.P. Microscale technologies for tissue engineering and biology. Proc Natl Acad Sci USA **103,** 2480, 2006.
5. Wobus, A.M., Wallukat, G., and Hescheler, J. Pluripotent mouse embryonic stem cells are able to differentiate into cardiomyocytes expressing chronotropic responses to adrenergic and cholinergic agents and Ca2+ channel blockers. Differentiation **48,** 173, 1991.
6. Xu, C., Police, S., Hassanipour, M., and Gold, J.D. Cardiac bodies: a novel culture method for enrichment of cardiomyocytes derived from human embryonic stem cells. Stem Cells Dev **15,** 631, 2006.
7. Gorelik, J., Ali, N.N., Shevchuk, A.I., Lab, M., Williamson, C., Harding, S.E., and Korchev, Y.E. Functional characterization of embryonic stem cell-derived cardiomyocytes using scanning ion conductance microscopy. Tissue Eng **12,** 657, 2006.
8. Martin, G.R., and Evans, M.J. Differentiation of clonal lines of teratocarcinoma cells: formation of embryoid bodies *in vitro*. Proc Natl Acad Sci USA **72,** 1441, 1975.
9. Martin, G.R., Wiley, L.M., and Damjanov, I. The development of cystic embryoid bodies *in vitro* from clonal teratocarcinoma stem cells. Dev Biol **61,** 230, 1977.
10. Ling, V., and Neben, S. *In vitro* differentiation of embryonic stem cells: immunophenotypic analysis of cultured embryoid bodies. J Cell Physiol **171,** 104, 1997.
11. Itskovitz-Eldor, J., Schuldiner, M., Karsenti, D., Eden, A., Yanuka, O., Amit, M., Soreq, H., and Benvenisty, N. Differentiation of human embryonic stem cells into embryoid bodies compromising the three embryonic germ layers. Mol Med **6,** 88, 2000.
12. Dang, S.M., Kyba, M., Perlingeiro, R., Daley, G.Q., and Zandstra, P.W. Efficiency of embryoid body formation and hematopoietic development from embryonic stem cells in different culture systems. Biotechnol Bioeng **78,** 442, 2002.
13. Karp, J.M., Yeh, J., Eng, G., Fukuda, J., Blumling, J., Suh, K.Y., Cheng, J., Mahdavi, A., Borenstein, J., Langer, R., and Khademhosseini, A. Controlling size, shape and homogeneity of embryoid bodies using poly(ethylene glycol) microwells. Lab Chip **7,** 786, 2007.
14. Bauwens, C.L., Peerani, R., Niebruegge, S., Woodhouse, K.A., Kumacheva, E., Husain, M., and Zandstra, P.W. Control of human embryonic stem cell colony and aggregate size heterogeneity influences differentiation trajectories. Stem Cells **26,** 2300, 2008.

15. Park, J., Cho, C.H., Parashurama, N., Li, Y., Berthiaume, F., Toner, M., Tilles, A.W., and Yarmush, M.L. Microfabrication-based modulation of embryonic stem cell differentiation. Lab Chip **7,** 1018, 2007.
16. Messana, J.M., Hwang, N.S., Coburn, J., Elisseeff, J.H., and Zhang, Z. Size of the embryoid body influences chondrogenesis of mouse embryonic stem cells. J Tissue Eng Regen Med **2,** 499, 2008.
17. Keller, G.M. *In vitro* differentiation of embryonic stem cells. Curr Opin Cell Biol **7,** 862, 1995.
18. Yamada, T., Yoshikawa, M., Kanda, S., Kato, Y., Nakajima, Y., Ishizaka, S., and Tsunoda, Y. *In vitro* differentiation of embryonic stem cells into hepatocyte-like cells identified by cellular uptake of indocyanine green. Stem Cells **20,** 146, 2002.
19. Moeller, H.C., Mian, M.K., Shrivastava, S., Chung, B.G., and Khademhosseini, A. A microwell array system for stem cell culture. Biomaterials **29,** 752, 2008.
20. Cameron, C.M., Hu, W.S., and Kaufman, D.S. Improved development of human embryonic stem cell-derived embryoid bodies by stirred vessel cultivation. Biotechnol Bioeng **94,** 938, 2006.
21. Carpenedo, R.L., Sargent, C.Y., and McDevitt, T.C. Rotary suspension culture enhances the efficiency, yield, and homogeneity of embryoid body differentiation. Stem Cells **25,** 2224, 2007.
22. Schroeder, M., Niebruegge, S., Werner, A., Willbold, E., Burg, M., Ruediger, M., Field, L.J., Lehmann, J., and Zweigerdt, R. Differentiation and lineage selection of mouse embryonic stem cells in a stirred bench scale bioreactor with automated process control. Biotechnol Bioeng **92,** 920, 2005.
23. deGennes, P.G., Brochard-Wyart, F., and Quéré, D. Capillarity and Wetting Phenomena: Drops, Bubbles, Pearls, Waves. New York: Springer, 2004.
24. Lamb, H. Statics, Including Hydrostatics and the Elements of the Theory of Elasticity. Cambridge, UK: Cambridge University Press, 1928.
25. Jones, G.E., and Starkey, R.L. Surface-active substances produced by *Thiobacillus thiooxidans*. J Bacteriol **82,** 788, 1961.
26. Croughan, M.S., Sayre, E.S., and Wang, D.I. Viscous reduction of turbulent damage in animal cell culture. Biotechnol Bioeng **33,** 862, 1989.
27. Foty, R.A., Forgacs, G., Pfleger, C.M., and Steinberg, M.S. Liquid properties of embryonic tissues: measurement of interfacial tensions. Phys Rev Lett **72,** 2298, 1994.
28. Padday, J.F., and Pitt, A.R. The stability of axisymmetric menisci. Proc R Soc Lond A **275,** 489, 1973.
29. Boucher, E.A., and Evans, M.J.B. Pendant drop profiles and related capillary phenomena. Proc R Soc Lond A **346,** 349, 1975.
30. Michael, D.H., and Williams, P.G. The equilibrium and stability of axisymmetric pendant drops. Proc R Soc London Ser A **351,** 117, 1976.
31. Chesters, A.K. An analytical solution for the profile and volume of a small drop or bubble symmetrical about a vertical axis. J Fluid Mech **81,** 609, 1977.
32. Michael, D.H. Meniscus stability. Ann Rev Fluid Mech **13,** 189, 1981.
33. Rio, O.I., and Neumann, A.W. Axisymmetric drop shape analysis: computational methods for the measurement of interfacial properties from the shape and dimensions of pendant and sessile drops. J Colloid Interface Sci **196,** 136, 1997.
34. Tada, S., Era, T., Furusawa, C., Sakurai, H., Nishikawa, S., Kinoshita, M., Nakao, K., and Chiba, T. Characterization of mesendoderm: a diverging point of the definitive endoderm and mesoderm in embryonic stem cell differentiation culture. Development **132,** 4363, 2005.
35. Walker, G.M., Ozers, M.S., and Beebe, D.J. Insect cell culture in microfluidic channels. Biomed Microdevices **4,** 161, 2002.
36. Abe, K., Niwa, H., Iwase, K., Takiguchi, M., Mori, M., Abe, S.I., and Yamamura, K.I. Endoderm-specific gene expression in embryonic stem cells differentiated to embryoid bodies. Exp Cell Res **229,** 27, 1996.
37. Roberts, C., Chen, C.S., Mrksich, M., Martichonok, V., Ingber, D.E., and Whitesides, G.M. Using mixed self-assembled monolayers presenting RGD and (EG)3OH groups to characterize long-term attachment of Bovine capillary endothelial cells to surfaces. J Am Chem Soc **120,** 6548, 1998.
38. Berthier, E., Warrick, J., Yu, H., and Beebe, D.J. Managing evaporation for more robust microscale assays. Part 2. Characterization of convection and diffusion for cell biology. Lab Chip **8,** 860, 2008.
39. Kurosawa, H., Imamura, T., Koike, M., Sasaki, K., and Amano, Y. A simple method for forming embryoid body from mouse embryonic stem cells. J Biosci Bioeng **96,** 409, 2003.
40. Kim, C., Lee, I.H., Lee, K., Ryu, S.S., Lee, S.H., Lee, K.J., Lee, J., Kang, J.Y., and Kim, T.S. Multi-well chip for forming a uniform embryoid body in a tiny droplet with mouse embryonic stem cells. Biosci Biotechnol Biochem **71,** 2985, 2007.
41. Ng, E.S., Davis, R.P., Azzola, L., Stanley, E.G., and Elefanty, A.G. Forced aggregation of defined numbers of human embryonic stem cells into embryoid bodies fosters robust, reproducible hematopoietic differentiation. Blood **106,** 1601, 2005.
42. Ezekiel, U.R., Muthuchamy, M., Ryerse, J.S., and Heuertz, R.M. Single embryoid body formation in a multi-well plate. Electron J Biotechnol **10,** 328, 2007.

Address correspondence to:
Ali Khademhosseini, Ph.D.
Harvard–MIT Division of Health Sciences and Technology
Massachusetts Institute of Technology
65 Landsdowne St., Rm 265
Cambridge, MA 02139

E-mail: alik@rics.bwh.harvard.edu

Received: April 14, 2009
Accepted: June 8, 2009
Online Publication Date: August 3, 2009

This article has been cited by:

1. Hao Qi, Guoyou Huang, Yu Long Han, Wang Lin, Xiujun Li, Shuqi Wang, Tian Jian Lu, Feng Xu. 2014. In vitro spatially organizing the differentiation in individual multicellular stem cell aggregates. *Critical Reviews in Biotechnology* 1-12. [CrossRef]
2. Anna Astashkina, David W. Grainger. 2014. Critical analysis of 3-D organoid in vitro cell culture models for high-throughput drug candidate toxicity assessments. *Advanced Drug Delivery Reviews* **69-70**, 1-18. [CrossRef]
3. Vincent H. B. Ho, Wei Mei Guo, Charlotte L. Huang, Shu Fen Ho, Su Yin Chaw, Ern Yu Tan, Kee Woei Ng, Joachim S.C. Loo. 2013. Manipulating Magnetic 3D Spheroids in Hanging Drops for Applications in Tissue Engineering and Drug Screening. *Advanced Healthcare Materials* **2**:11, 1430-1434. [CrossRef]
4. Sasha Cai Lesher-Perez, John P. Frampton, Shuichi Takayama. 2013. Microfluidic systems: A new toolbox for pluripotent stem cells. *Biotechnology Journal* **8**:2, 180-191. [CrossRef]
5. Yuya Morimoto, Shoji Takeuchi. 2013. Three-dimensional cell culture based on microfluidic techniques to mimic living tissues. *Biomaterials Science* **1**:3, 257. [CrossRef]
6. Yong Park, Woo Young Sim, Won Gu Lee. 2012. A controllable liquid mold for fabrication of 3D spherical structures and arrays. *Microsystem Technologies* . [CrossRef]
7. Amy Y. Hsiao, Yi-Chung Tung, Chuan-Hsien Kuo, Bobak Mosadegh, Rachel Bedenis, Kenneth J. Pienta, Shuichi Takayama. 2011. Micro-ring structures stabilize microdroplets to enable long term spheroid culture in 384 hanging drop array plates. *Biomedical Microdevices* . [CrossRef]
8. Yi-Chung Tung, Amy Y. Hsiao, Steven G. Allen, Yu-suke Torisawa, Mitchell Ho, Shuichi Takayama. 2011. High-throughput 3D spheroid culture and drug testing using a 384 hanging drop array. *The Analyst* **136**:3, 473. [CrossRef]
9. Amy Y. Hsiao, Yi-Chung Tung, Xianggui Qu, Lalit R. Patel, Kenneth J. Pienta, Shuichi Takayama. 2011. 384 hanging drop arrays give excellent Z-factors and allow versatile formation of co-culture spheroids. *Biotechnology and Bioengineering* n/a-n/a. [CrossRef]
10. Diep Nguyen, Silin Sa, Jonathan D. Pegan, Brent Rich, Guangxin Xiang, Kara E. McCloskey, Jennifer O. Manilay, Michelle Khine. 2009. Tunable shrink-induced honeycomb microwell arrays for uniform embryoid bodies. *Lab on a Chip* **9**:23, 3338. [CrossRef]